

von Willebrand factor promotes platelet-induced metastasis of osteosarcoma through activation of the VWF-GPIIb axis

Q. Wang^{a,c,1}, W. Liu^{c,1}, J. Fan^{d,1}, J. Guo^e, F. Shen^{a,b}, Z. Ma^{a,b}, C. Ruan^{a,b}, L. Guo^c, M. Jiang^{a,b,*}, Y. Zhao^{a,b,*}

^a Jiangsu Institute of Hematology, Key Laboratory of Thrombosis & Hemostasis of Ministry of Health, The First Affiliated Hospital of Soochow University, Suzhou 215006, China

^b Collaborative Innovation Center of Hematology, Soochow University, Suzhou 215006, China

^c Pathology Department, The First Affiliated Hospital of Soochow University, Suzhou 215006, China

^d Stomatology Department, The Second Affiliated Hospital of Soochow University, Suzhou, 215004, China

^e Orthopedics Department, The First Affiliated Hospital of Soochow University, Suzhou 215006, China

ARTICLE INFO

Keywords:

VWF
Osteosarcoma
Platelet
Metastasis

ABSTRACT

von Willebrand factor (VWF) is exclusively expressed in endothelial cells (ECs) and megakaryocytes, which plays a crucial role in the initiation of arterial thrombosis. Recent studies have shown that VWF is also expressed in osteosarcoma (OS) cells and participates in adhesion of cancer cells to platelets, thus promoting metastasis of OS cells. However, it is unclear how OS cell-derived VWF-platelet interaction contributes to the metastasis of OS. We hypothesized that the interaction is mediated by the binding between VWF A1 and GPIIb/IIIa of platelets, a molecular mechanism similar to that of thrombosis. The increased expression of VWF in SAOS2 cells may contribute to the enhancement of platelet adhesion through the VWF-GPIIb pathway, which could promote the migration and invasion capacities of SAOS2 cells in vitro. Antibodies that block the pathway could significantly inhibit the platelet-induced metastasis of OS cells. Our results suggest a theoretical basis for the development of new anti-OS metastasis drugs, and further enrich the mechanism of OS metastasis.

1. Introduction

von Willebrand factor (VWF) is a multimeric glycoprotein that plays a pivotal role in hemostasis and thrombosis. Commonly, VWF is exclusively expressed in endothelial cells (ECs) and megakaryocytes, which can be released to plasma in the form of multimer under certain stimulating conditions [1–3]. However, it was reported that VWF was also detected in some cancer cells of non-endothelial origin, such as glioma and osteosarcoma (OS) [4]. Although the analyses demonstrated the mechanism of transcriptional activation of the VWF in cancer cells was consistent with that in ECs [4], the differential expression form of VWF in ECs and cancer cells still remains unclear.

Discordant with most investigations focused on the ECs and platelets as the source of VWF [5], a few studies have found that VWF could

participate in modulating OS metastasis that was affected by the expression of VWF in OS cells [4,6]. Furthermore, these analyses also indicated that the overexpressed VWF could enhance the metastatic potential of OS cells by adhering to more platelets. VWF knock down decreased the adhesion, transmigration and extravasation capacities of OS cells. However, the detailed mechanism that how OS cell-derived VWF interacts with platelets contributing to the cancer metastasis remains to be elucidated.

In the classic hemostasis process, multimer VWF is a bridge between the collagen matrix and platelets. The binding of VWF to the platelets glycoprotein IIb/IIIa (GPIIb/IIIa) mediates the adhesion of platelets to collagen in the exposed subendothelial matrix of damaged blood vessels [7]. Thus, the collagen-VWF-GPIIb axis plays an important role in thrombus formation [8,9]. Due to the large amount of collagen [10–13] and

Abbreviations: VWF, von Willebrand factor; OS, Osteosarcoma; GPIIb, Glycoprotein IIb; ECs, Endothelial cells; FBS, Fetal bovine serum; FITC, Fluorescein isothiocyanate; mAb, Monoclonal antibody; PFA, Paraformaldehyde; CFSE, 5-(6)-carboxyfluorescein succinimidyl ester; ELISA, Enzyme-linked immunosorbent assay; H&E, Hematoxylin and eosin; PMA, Phorbol 12-myristate 13-acetate; WPB, Weibel-Palade body; UL-VWF, Ultra-large multimer VWF

* Corresponding authors at: Jiangsu Institute of Hematology, The First Affiliated Hospital of Soochow University, Key Laboratory of Thrombosis and Haemostasis, Ministry of Health, 188 Shizi Street, Suzhou 215006, China.

E-mail addresses: jiangmiao@suda.edu.cn (M. Jiang), zhaoyimingbox@163.com (Y. Zhao).

¹ These authors contributed equally to this work.

<https://doi.org/10.1016/j.jbo.2020.100325>

Received 22 April 2020; Received in revised form 1 September 2020; Accepted 21 September 2020

Available online 08 October 2020

2212-1374/ © 2020 The Authors. Published by Elsevier GmbH. This is an open access article under the CC BY-NC-ND license (<http://creativecommons.org/licenses/by-nc-nd/4.0/>).

expression of VWF in OS cells, we hypothesized the collagen-VWF-GPIb axis is one of the most likely pathway that mediates the OS-platelets interactions. In order to confirm the hypothesis, we used the advanced OS cell line SAOS2 as a cell model to examine the expression form of VWF in tumor cells and explore the interaction between tumor cell-derived VWF and platelets. A variety of VWF-GPIb pathway blocking antibodies were used to investigate the inhibition effects on platelets adhesion, migration and invasion capacities of OS cells. These results help to detect a new therapeutic target that can inhibit the metastasis of OS.

2. Materials and methods

2.1. Patients and specimens

All paraffin-embedded specimens were obtained from 7 OS patients (5 male and 2 female; mean age, 18 years; age range, 10–34 years) undergoing surgery at the First Affiliated Hospital of Soochow University between January 2010 to December 2019. None of the patients had received any preoperative treatment. All of these patients had histologically-confirmed metastasis. The OS specimens were subclassified as primary OS ($n = 7$), invasive OS ($n = 7$), and lung metastases ($n = 7$). These three types of specimens are collected at the same time from three different regions of OS in the same patient. Tumors that confined to the periosteum of the primary site is defined as primary OS, while tumors breaking out to the periosteum and invading the surrounding soft tissue is defined as invasive OS. Lung metastases refer to lung metastasis of OS. All studies were approved by the ethics committee of the First Affiliated Hospital of Soochow University in Suzhou, China and the ethical standards of the 1964 Declaration of Helsinki. All the patients all signed the informed consent.

2.2. Hematoxylin and eosin staining

Center of the specimens of primary OS ($n = 7$), invasive OS ($n = 7$), and lung metastases ($n = 7$) were fixed in 4% paraformaldehyde (PFA) and embedded in paraffin. One glass slide was prepared for each specimen for H&E staining. Placing the glass slides that hold the paraffin sections in staining racks. Clearing the paraffin from the samples in three changes of xylene for 2 min per change. Transferring the slides through 100%, 95%, 70% ethanol for 2 min per change. Rinsing the slides in running tap water at room temperature for at least 2 min. Staining the samples in hematoxylin solution for 3 min. Placing the slides under running tap water at room temperature for at least 5 min. Staining the samples in working eosin Y solution for 2 min. Dipping the slides in 95% ethanol about 20 times. Transferring to 95% ethanol for 2 min. Transferring through two changes of 100% ethanol for 2 min per change. Clearing the samples in three changes of xylene for 2 min per change. Placing a drop of Permount over the tissue on each slide and add a coverslip. Viewing the slides using a microscope.

2.3. Immunohistochemistry

Center of the specimens of primary OS ($n = 7$), invasive OS ($n = 7$), and lung metastases ($n = 7$) were fixed in 4% PFA and embedded in paraffin. One glass slide was prepared for each specimen for immunohistochemistry analysis. Sections (4 μm) were incubated with the anti-VWF mouse anti-human monoclonal antibody (mAb) SZ34 (2 $\mu\text{g}/\text{mL}$) overnight at 4 °C, then with multiuse secondary antibody (1:1000 dilution, Dako, UK). Staining was treated with an Envision + kit (MBX, Fuzhou, China) for 30 min and automatically stained using a Discovery XT Ventana autostainer following damasking procedures to retrieve antigens. Five high-power (200 \times) fields were randomly selected for each sample. The final staining score was determined by the VWF-positive tumor cell rate and categorized into four semi-quantitative classes: – (0% positive cells), + (1–2% positive cells), ++ (2–4%

positive cells) and +++ (4–10% positive cells). The positivity was evaluated in only tumor cells, and normal bone and ECs were not included in this evaluation.

2.4. Cell lines and cell culture

The human OS cell line SAOS2 and MG63 and the human embryonic kidney cell line HEK293 were purchased from Hengtong BioTECH (Jinan, China) and cultured in McCoy's 5A media (Procell, Wuhan, China) and Dulbecco's modified Eagle's medium (DMEM, HyClone, Logan, Utah, America) containing 10% fetal bovine serum (FBS) (Gibco, Carlsbad, USA) at 37 °C in a humidified 5% CO₂ incubator. Human microvascular endothelial cells (HMEC-1) were obtained from the Central Laboratory, Soochow University, China and maintained according to the manufacturer's protocol.

2.5. Western blot analysis

SAOS2, MG63, HMEC-1, HEK293 and human washed platelets were lysed in SDS sample buffer (Beyotime Biotechnology, Shanghai, China) and separated on a 6% sodium dodecyl sulfate (SDS)-polyacrylamide gel followed by transfer to a nitrocellulose membrane (Amersham Pharmacia Biotech AB). After blocking with 5% skim milk in 0.1% PBST overnight at 4 °C, the membrane was incubated with the anti-VWF mouse anti-human mAb SZ123 (3 $\mu\text{g}/\text{mL}$ in PBS + 0.1% Tween 20) for two hours at room temperature. The specifically bound primary mAb was then detected with HRP-conjugated goat anti-mouse IgG (Immunotech, Marseille, France) for an hour. After extensive washing, proteins were visualized by enhanced chemiluminescence (ECL; Sigma-Aldrich, St. Louis, MO, USA).

2.6. PMA stimulates SAOS2 cells to express VWF

SAOS2 cells (1 $\times 10^6$ cells/mL) were seeded into dishes (35 \times 10 mm, Corning, New York, NY, USA) and allowed to attach overnight. 50 ng/mL phorbol 12-myristate 13-acetate (PMA, Alexis Biochemicals, San Diego, CA) was incubated with the SAOS2 cells for 12 h, and then the cells were washed twice using phosphate-buffered saline (PBS). Subsequently, cells were fixed with 4% PFA for 10 min to fix the cells and punch holes in the cell membrane to make the antibody easier to penetrate. Then the SAOS2 cells were labeled with Hoechst 33342 (Sigma-Aldrich, USA) and stained for VWF with fluorescein isothiocyanate (FITC)-conjugated anti-VWF polyclonal antibody (polyAb) according to the manufacturer's protocol. After that, the dishes were imaged using confocal laser endomicroscopy (CLE; LEICA DC300, LEICA DMIRB, Wetzlar, Germany) imaging with the same lighting exposure time of 90 s.

2.7. VWF multimer electrophoresis analysis

VWF multimers were separated by electrophoresis using 1.0% agarose gel under reducing conditions. Sample buffer (0.5 M Tris-HCl [pH 6.8], 0.5 M EDTA, 9 M Urea, 20%SDS) was used to dilute the sample. Electrophoresis was under 4 °C at 90 V for 4 h, and was transferred to the agarose gel support medium (Lonza, USA) overnight. 3% non-fat milk was used for blocking, and subsequently the agarose gel support medium was incubated with HRP-rabbit anti-human (RAH) VWF IgG for 1.5 h at room temperature. Separate bands were visualized by chemiluminescence to show various VWF multimeric form.

2.8. Flow cytometry studies

Cultured SAOS2 and MG63 cells were incubated with 50 ng/mL PMA for 12 h and then washed twice using PBS. Subsequently, cells (5 $\times 10^5$ cells/mL) pretreated with or without PMA were collected by trypsin-EDTA treatment and fixed with 4% PFA followed by staining

with FITC-conjugated anti-VWF polyAb (2 µg/tube) for 30 min at room temperature. After diluting 3-fold with PBS, samples were analyzed with FACSCalibur (BD Biosciences, San Jose, CA, USA).

2.9. Preparation of washed human platelets

Blood was drawn from healthy volunteers, 1:7 mixed with acid-citrate-dextrose (ACD), and then centrifuged at 150g for 20 min. Platelet-rich plasma (PRP) was collected and centrifuged at 800 g for 10 min. Following that, platelets were then washed three times in CGS buffer (14.7 mM trisodium citrate, 33.33 mM glucose and 123.2 mM NaCl, pH 7) and supplemented with CaCl₂/MgCl₂ buffer prior to experimentation.

2.10. Platelet adhesion to SAOS2 cells under static conditions

SAOS2 cells (1 × 10⁶ cells/mL) were seeded into dishes and treated with PMA as described above. After washing twice using PBS, VWF was stained with SZ34 (anti-VWF mAb) labeled with Alexa Fluor 555 for 1 h. Then, cells were preincubated with or without mouse-IgG, the anti-VWF mAbs SZ123 (mAb targeting the A3 domain of VWF) and AVW3 (mAb targeting the A1 domain of VWF) (GTI, Brookfield, WI, USA) (10 µg/ml) for 15 min at 37 °C. Washed platelets were preincubated with or without mouse-IgG and the anti-GPIbα mAb SZ2 (mAb targeting the platelet GPIb) (10 µg/mL). After that, one hundred microliters of the washed platelets (1 × 10⁷ platelets/mL) stained with Calcein-AM (1:1,000 L/L, Dojindo, Japan) were added to the dishes and cocultured with the SAOS2 cells under static conditions for 30 min. The platelets were washed twice using PBS to remove the non-adherent platelets. Then, the SAOS2 cells were labeled with Hoechst 33,342 as described above. CLE imaging was carried out with an excitation wavelength of 488 nm and an emission wavelength of 505–585 nm. The area covered by the platelets was measured and calculated by an image analysis system (SigmaScan Pro4.0; Jandel Scientific, San Rafael, CA, USA). Platelet adhesion was recorded as the percentage of the surface covered by the platelets in five separate microscopic fields at 100 × magnification and expressed as the mean ± SD (n = 3).

2.11. Platelet adhesion to SAOS2 cells under shear flow conditions

SAOS2 cells (2.5 × 10⁵ cells/mL) were seeded onto microscope slides (Sigma-Aldrich, USA) at 37 °C and allowed to attach overnight. After pretreating with PMA as described above, the SAOS2 cells were preincubated with mouse-IgG followed by the anti-VWF mAbs SZ123 and AVW3 (GTI, Brookfield, WI, USA) (50 µg/ml) for 15 min at 37 °C. Whole blood (low-molecular-weight heparin was used as an anticoagulant, 40 U mL⁻¹) stained with Calcein-AM (1:1,000, L/L) was preincubated with mouse-IgG and the anti-GPIbα mAb SZ2 (50 µg/ml). Perfusion was carried out under a shear rate of 1,000 s⁻¹ in a parallel-plate flow chamber (GlycoTech, Maryland, USA). During the perfusion, the platelets adhered on the cell-coated surface were evaluated with a light microscope (LEICA DC300, LEICA DMIRB, Wetzlar, Germany) at 2, 5, 10 and 15 min. The adherent platelets were quantified as described above.

2.12. Tumor cell migration and invasion assay

SAOS2 and MG63 cells (2.5 × 10⁵ cells/mL) pretreated with PMA were resuspended in McCoy's 5A medium and DMEM without FBS. Cells were preincubated with or without SZ123 and AVW3 (10 µg/mL) and platelets were preincubated with or without SZ2 (10 µg/mL). Then, the cells alone or a 1:1 mixture of the cells with platelets (5 × 10⁶ platelets/mL) were added to the upper compartment of 24-well Transwell culture dishes (Costar Corporation, Cambridge, MA). Subsequently, 500 µL medium were added to the lower chamber. The chamber was put into the carbon dioxide incubator and cultured for

12 h. The next day, the cells were washed twice using PBS, fixed with 4% PFA and then stained with 5-(6)-carboxyfluorescein succinimidyl ester (CFSE, 1:1,000, Dojindo). The nontransmigrated cells in the upper compartment were removed, and only the transmigrated cells on the lower side of the filter or the bottom of the Transwell were imaged (Zeiss Axio Observer.Z1 and Olympus IX81) and quantified.

The invasion assay was based on the Transwell cell migration assay. A total of 100 µL Matrigel (BD Biosciences, diluted with the appropriate serum-free medium at a ratio of 1:6) was added to the upper membranes. All assays were performed in triplicate.

2.13. Statistical analyses

Statistical analysis was performed using SPSS 19.0 statistical software (SPSS, Chicago, IL, USA). Data were given as the mean ± SD, and statistical analyses were performed with Student's *t* test (paired) or one-way ANOVA followed by Fisher's test. Statistically significant changes (p < 0.05) between groups are marked by asterisks (*).

3. Results

3.1. Expression of VWF in human OS tissue specimens

We first used hematoxylin and eosin (H&E) and immunohistochemistry to investigate VWF protein levels in 21 OS specimens of 7 OS patients. Immunohistochemical analysis showed that the expression level of VWF was significantly higher in the metastatic than in the non-metastatic OS samples (Table 1, Fig. 1A, B and C). Moreover, rates of VWF-positive tumor cell were higher in the invasive and lung metastatic (5.22% and 5.38%, respectively) than in the primary (1.38%) OS samples (Fig. 1D, ***P < 0.001).

3.2. PMA can stimulate SAOS2 cells to secrete and release VWF

VWF expression was detected in SAOS2 cells, HMEC-1 cells and platelet lysates (positive control) but not in HEK293 cells or MG63 cells by Western blotting (Fig. 2A). The intensity of the immunofluorescence staining for VWF expression in SAOS2 cells treated with PMA (50 ng/ml, 12 h) was much stronger than that in untreated cells (Fig. 2B). Western blotting performed for the immunofluorescence staining also showed similar results of SAOS2 cells while there was no significant difference in the levels of VWF expression between the negative control MG63 cells treated with or without PMA (50 ng/ml, 12 h) (Fig. 2C). In addition, flow cytometric analysis also indicated that the levels of VWF expressed on the cell membrane in SAOS2 cells treated with PMA were significantly higher than those in the untreated cells while the negative control MG63 cells not (Fig. 2D). In SAOS2 cells, VWF is more likely to be present in the form of medium molecular weight polymers, whereas VWF polymers of ultra molecular weights are expressed in HMEC-1 (Fig. 2E).

3.3. Overexpressed VWF promotes adhesion of SAOS2 cells to platelets through the VWF-GPIb pathway

The levels of VWF on the cell membrane in the cells treated with PMA were significantly higher than those in the untreated cells (Fig. 3A and B, ***P < 0.001). The SAOS2 cells treated with PMA exhibited a significantly higher platelet adhesion capacity than the cells not treated with PMA. When the AVW3 (mAb targeting the A1 domain of VWF) and SZ123 (mAb targeting the A3 domain of VWF) and the SZ2 (mAb targeting the platelet GPIb) were added to the culture to block the interaction between VWF and platelets, we found that there were significant reductions in the platelet adhesiveness of the SAOS2 cells treated with AVW3 and the platelets treated with SZ2 (Fig. 3A and C, ***P < 0.001).

To explore the adhesion ability of SAOS2 cells under physiological

Table 1
Clinical features of human tissue specimens employed for the evaluation of VWF expression.

Case No.	Gender	Age(years)	Position	Primary tumor site	Maximum primary tumor size, cm*	Lung involvement	No. of lung nodules	VWF
1	M	19	Primary OS Invasive OS Lung metastases	Femur	5.9	Right lung only	1	+ ++ ++
2	M	14	Primary OS Invasive OS Lung metastases	Below knee	12.3	Both lungs	5	+ ++ +++
3	F	34	Primary OS Invasive OS Lung metastases	Pelvis	8.2	Right lung only	1	++ ++ ++
4	F	10	Primary OS Invasive OS Lung metastases	Below knee	13.4	Left lung only	3	+ ++ ++
5	M	13	Primary OS Invasive OS Lung metastases	Femur	9.6	Both lungs	3	+ + ++
6	M	16	Primary OS Invasive OS Lung metastases	Humerus	10.6	Both lungs	2	++ +++ +++
7	M	21	Primary OS Invasive OS Lung metastases	Femur	10.5	Left lung only	2	+ ++ ++

conditions, a laminar shear flow chamber was used to allow platelet flow over the surface of SAOS2 cells. In these analyses, the SAOS2 cells were either untreated or treated with PMA and pretreated with mAbs, SZ123 or AVW3. Under shear stress, the SAOS2 cells treated with PMA formed clumps (cell-platelet hetero-aggregates) that were larger in size and number than those formed by the cells not treated with PMA. The mAbs SZ2 and AVW3 could inhibit platelet adhesion to SAOS2 cells under the shear flow conditions (Fig. 4, $***P < 0.001$). Interestingly, SZ123 also had the same effect as SZ2 and AVW3 under the shear flow conditions, which was different from its effect under the static conditions.

3.4. VWF-platelet interaction promotes transmigration and invasion capacities of SAOS2 cells through the VWF-GPIIb pathway

We next performed transwell migration and invasion assays and using antibodies that block the VWF-GPIIb pathway to gain insight into how VWF-platelet interaction contributes to the metastasis of OS. For the transwell migration assay, the number of transmigrated SAOS2 cells pretreated with PMA and co-cultured with platelets was significantly higher than without platelets. Furthermore, we found that the number of transmigrated SAOS2 cells was significantly decreased when the cells were pretreated with AVW3 or the platelets were pretreated with SZ2, whereas SZ123 did not have the same effect. As a control, there was no significant difference in the amount of transmigrated MG63 cells between those co-cultured with and without platelets (Fig. 5A and C, $**P < 0.01$, $***P < 0.001$). Consistent with migration assay, the results of the invasion assay also showed that the capacity of SAOS2 cells that penetrate the matrigel could be enhanced when co-cultured with platelets and inhibited by mAbs AVW3 and SZ2 in contrast of results of MG63 cells (Fig. 5B and D, $***P < 0.001$).

4. Discussion

OS, which is a highly metastatic cancer, is the most common malignant bone tumor, and pulmonary metastasis is the most common cause of death in OS patients [14,15]. With the improvement of medical technology in recent years, the long-term survival of patients with nonmetastatic OS has significantly improved, and the 5-year survival rate has exceeded 70%. However, once OS metastasizes, the 5-year survival rate is only approximately 20% [16]. Thus, the development of efficient approaches to discover potential compounds that target the metastasis of OS remains a topic of considerable interest [17–20].

VWF has been reported to be expressed in OS cells in recent studies. Consistent with the analyses that revealed an increase in VWF gene expression in OS metastases [6], our immunohistochemistry results first directly showed that the expression level of VWF was significantly higher in lung metastatic and invasive than in the non-metastatic OS cells in pathological specimens. Thus, it was clearly confirmed that the OS cell-derived VWF could increase during tumor progression and contribute to the metastasis of OS. In order to further investigate its role in cancer metastasis, we next studied its expression form in OS cells. Our results demonstrated that it was mainly expressed as low molecular weight multimer in OS cell line SAOS2, in contrast to ultralarge weight multimer of VWF (UL-VWF) in ECs. Based on these results, it was hypothesized that the OS cell-derived VWF could be synthesized and secreted faster under inflammatory factor-stimulated conditions.

In the process of tumor metastasis, cancer cells need to adjust to various changes in pericellular environment. These changes include the secretion of multiple adhesion molecules [21]. As a powerful inflammatory factor, PMA can play a significant role in promoting differentiation [22] and has been reported to induce the release of Weibel-Palade body (WPB)-stored VWF in ECs. Based on these studies, our experiment used 50 $\mu\text{g}/\text{ml}$ PMA to stimulate SAOS2 cells for 12 h. After treatment, the VWF expression in the cell membrane was increased significantly and the overexpressed VWF OS cell model was successfully

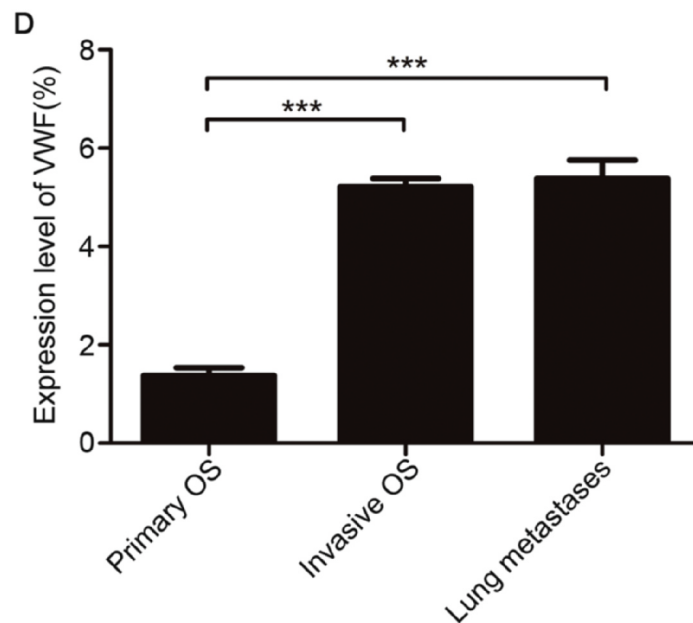
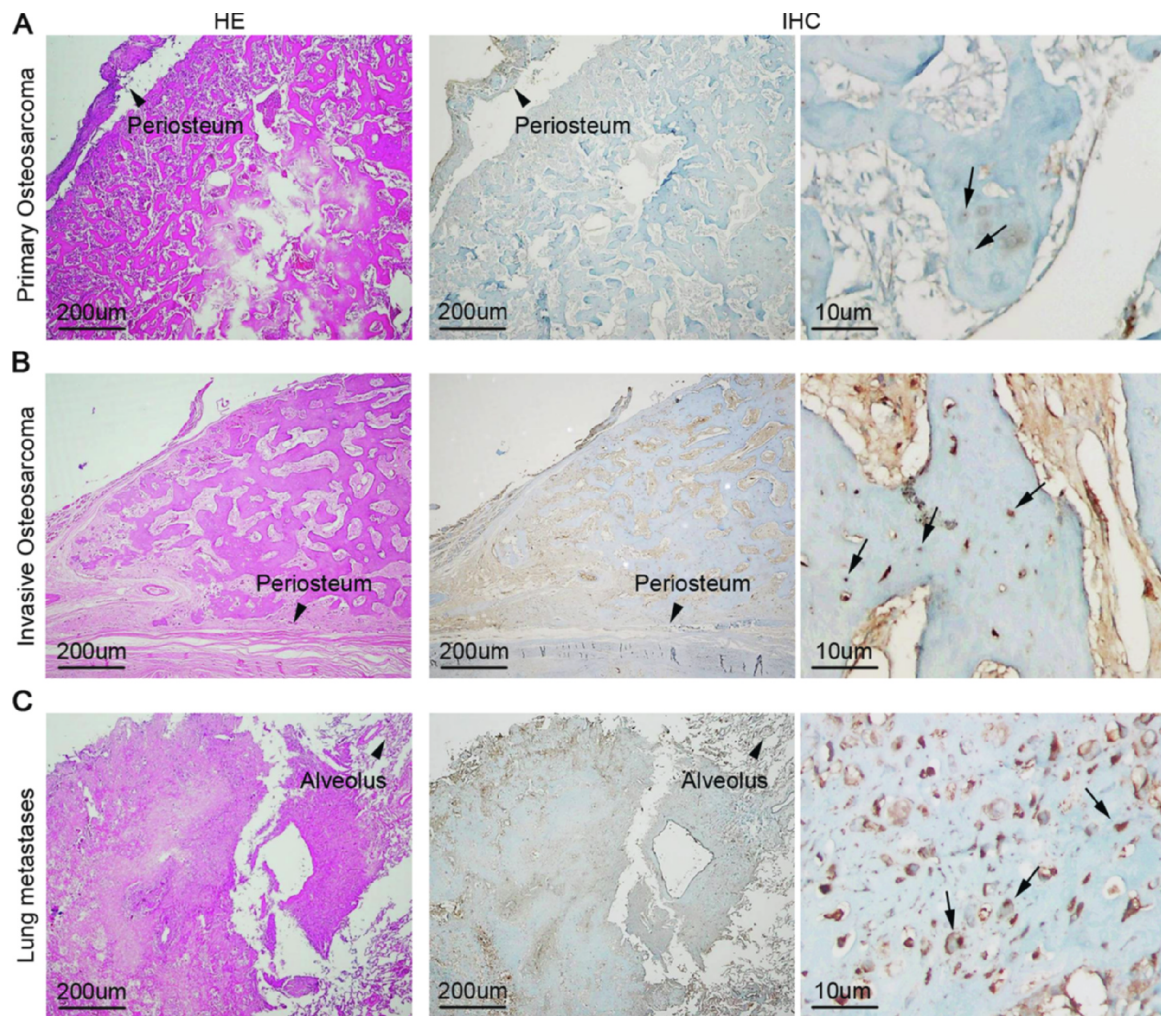


Fig. 1. VWF was more highly expressed in metastatic compared to primary tumor specimens. (A) Low expression of VWF in primary osteosarcoma (n = 7); (B) high expression of VWF in invasive osteosarcoma (n = 7); (C) high expression of VWF in osteosarcoma with lung metastases (n = 7); (D) quantification of VWF expression in three types of osteosarcoma specimens. Mean ± SD is shown for five high-power fields of view/sample. ***P < 0.001.

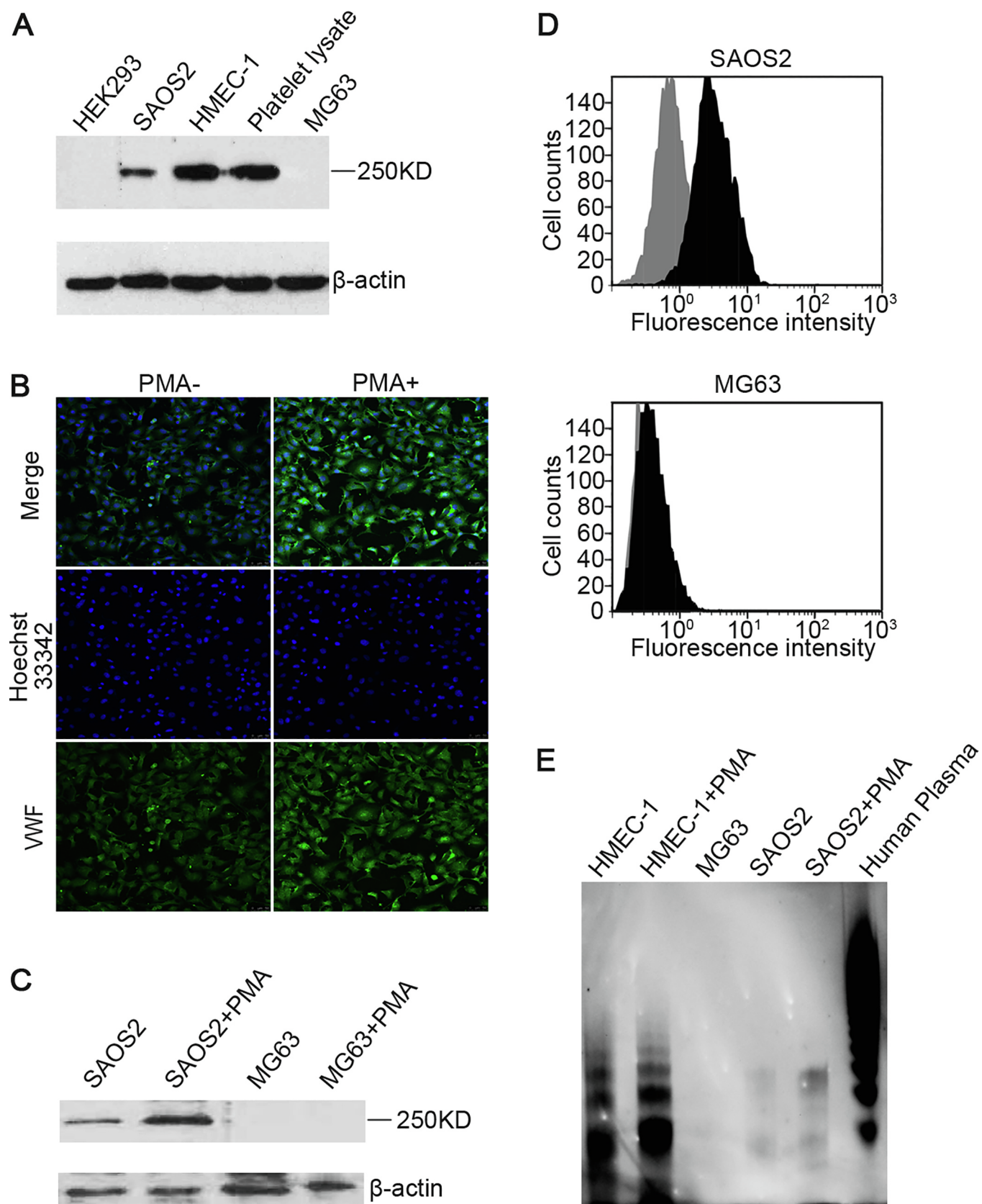


Fig. 2. PMA stimulated SAOS2 cells to secrete and release VWF. (A) SAOS2 and MG63 cell lysates were used in immunoblotting assay. HMEC-1 and platelet lysates were used as positive controls. HEK293 was used as a negative control; (B) immunofluorescence staining detected VWF expression level in SAOS2 cells treated with or without PMA. Hoechst 33342 staining (blue) marked the nucleus. VWF (green) was stained with FITC-conjugated anti-VWF polyAb; (C) SAOS2 and MG63 cell treated with or without PMA were used in immunoblotting assay; (D) flow cytometric analyses of VWF expressed on the surface of SAOS2 cells treated with or without PMA, MG63 was used as a negative control; (E) VWF multimeric structure in SAOS2 and HMEC-1 cells treated with or without PMA, human plasma and MG63 cells was analyzed by agarose gel electrophoresis. Separate bands were visualized by chemiluminescence to show various sizes of VWF molecular. (For interpretation of the references to colour in this figure legend, the reader is referred to the web version of this article.)

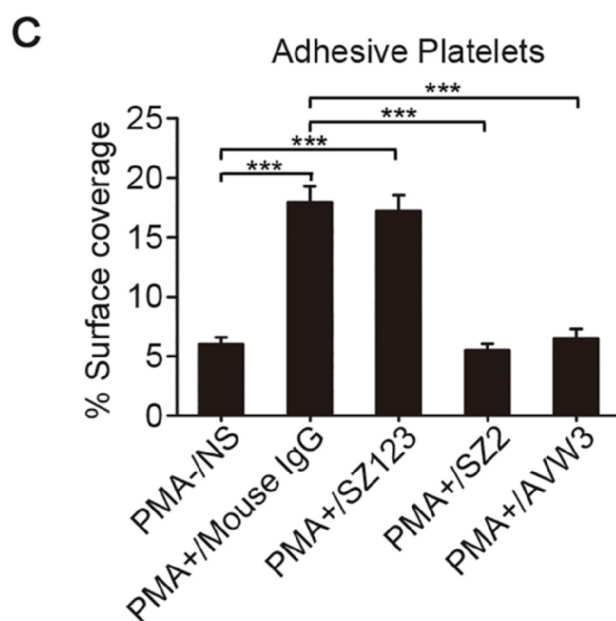
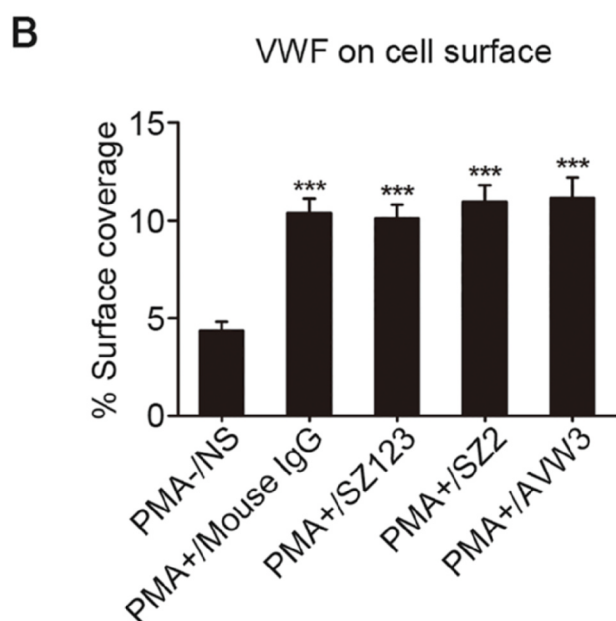
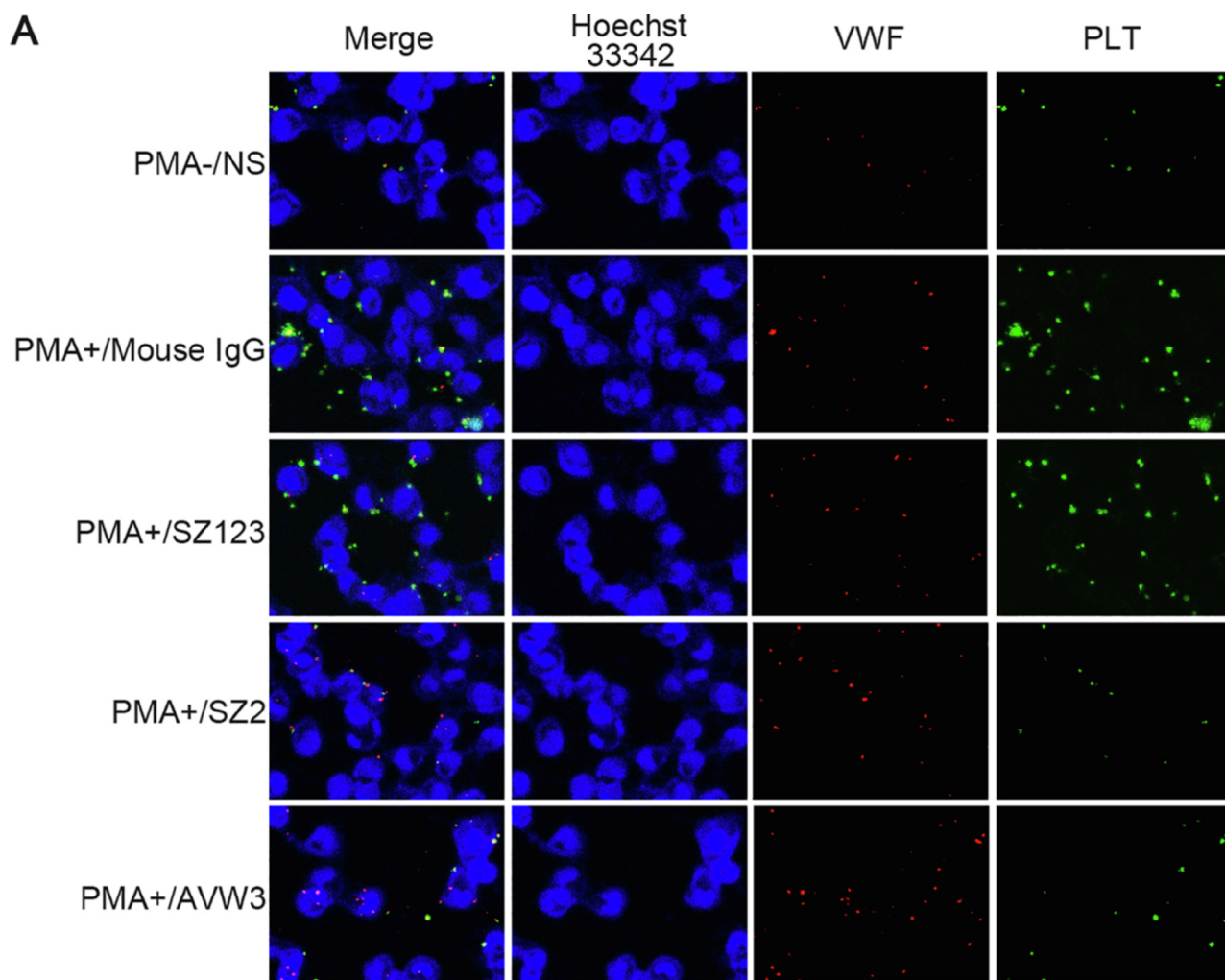


Fig. 3. Inhibition effect of VWF-GPIb pathway blocking antibodies in platelets adhesion assay. (A) Platelets adhesion assay was performed on PMA-/NS, PMA + / Mouse IgG, PMA + /SZ123, PMA + /SZ2 and PMA + /AVW3. Platelets (green) were treated with staining reagent Calcein-AM. SAOS2 cells (blue) were labeled with cytoplasmic staining reagent Hoechst 33342. VWF (red) was stained with mAb SZ-34 for visualization; (B) quantification of VWF expressed on the surface of SAOS2 cells in PMA-/NS, PMA + /Mouse IgG, PMA + /SZ123, PMA + /SZ2 and PMA + /AVW3. ***P < 0.001; (C) quantification of surface covered by adherent platelets to SAOS2 cells in PMA-/NS, PMA + /Mouse IgG, PMA + /SZ123, PMA + /SZ2 and PMA + /AVW3. ***P < 0.001. Mean ± SD is shown for three separate experiments. (For interpretation of the references to colour in this figure legend, the reader is referred to the web version of this article.)

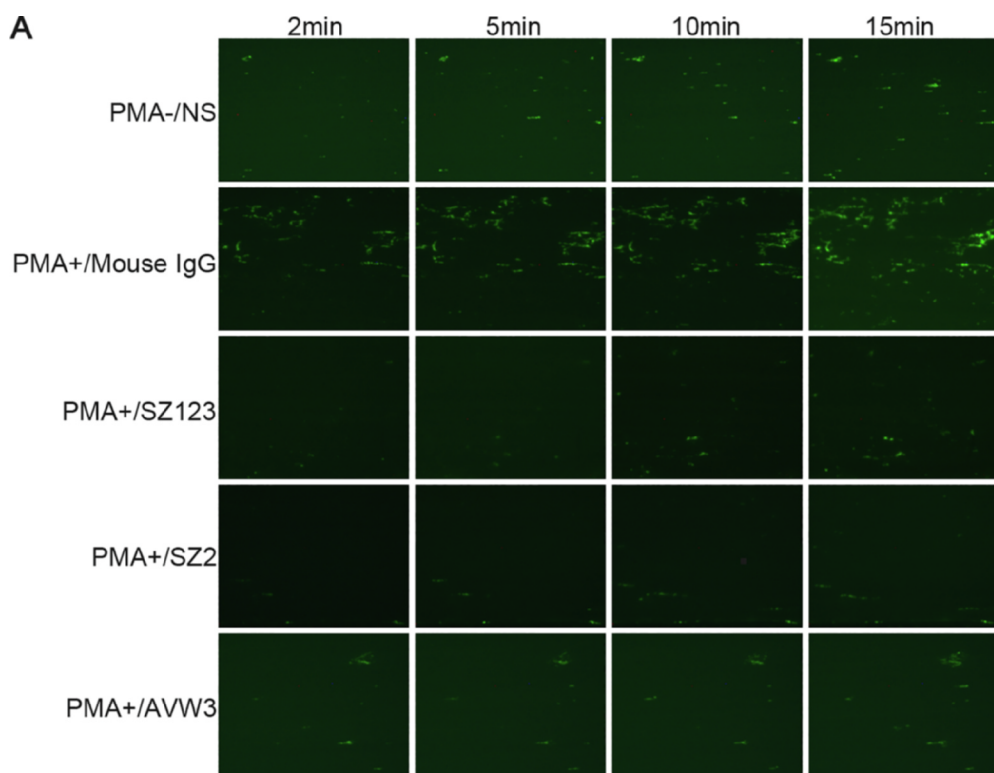
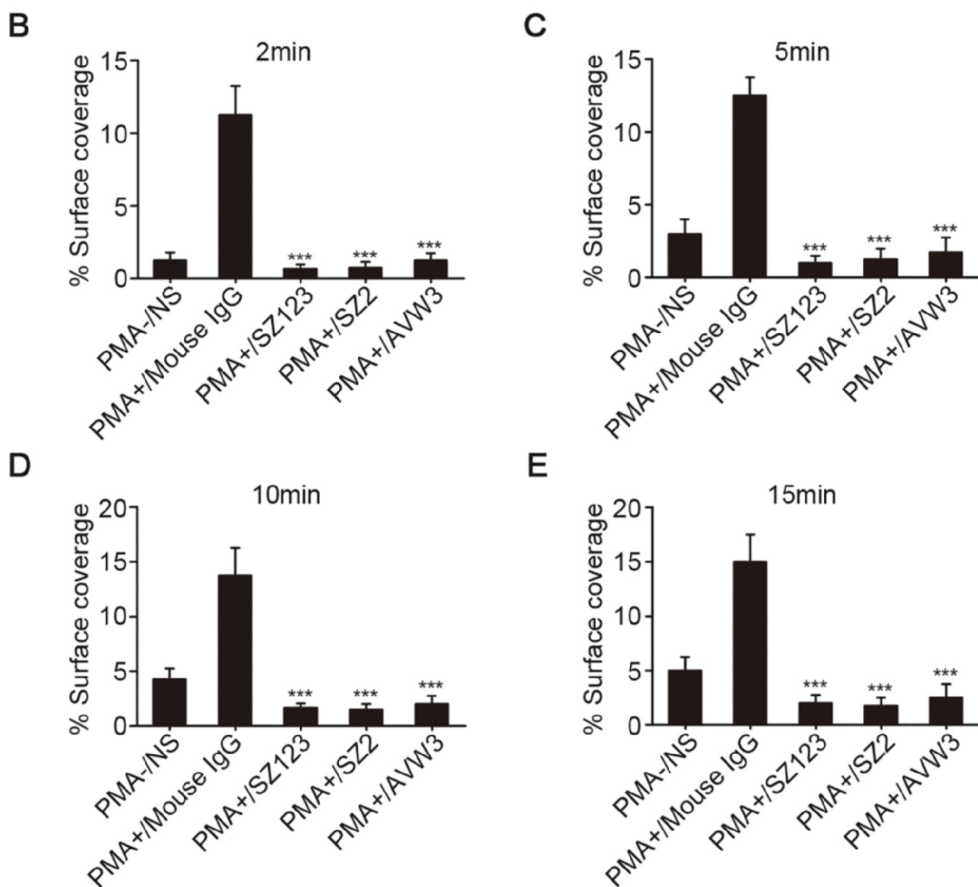


Fig. 4. Inhibition effect of VWF-GPIb pathway blocking antibodies in platelets adhesion assay under shear stress. (A) the microscopic images of heparinized whole blood stained with Calcein-AM (green) perfused over SAOS2 cells at a constant high shear rate of 1000/s for 15 min in PMA-/NS, PMA+/Mouse IgG, PMA+/SZ123, PMA+/SZ2 and PMA+/AVW3. ***P < 0.001; (B)–(E) quantification of surface covered by adherent platelets to SAOS2 cells in PMA-/NS, PMA+/Mouse IgG, PMA+/SZ123, PMA+/SZ2 and PMA+/AVW3 at 2, 5, 10 and 15 min. ***P < 0.001. Mean ± SD is shown for three separate experiments. (For interpretation of the references to colour in this figure legend, the reader is referred to the web version of this article.)



obtained. We hypothesized that consistent with the effect on Ecs, PMA may induce translocation of VWF from cytoplasmic domain of SAOS2, potentially induce the secretion, and released VWF may associate with the cell membrane.

It has been well established that platelets bound to tumor cells may protect the tumor cells from immune surveillance and promote the adhesion of the tumor cells to leukocytes and the endothelium, thereby enhancing both extravasation from the vasculature and distant

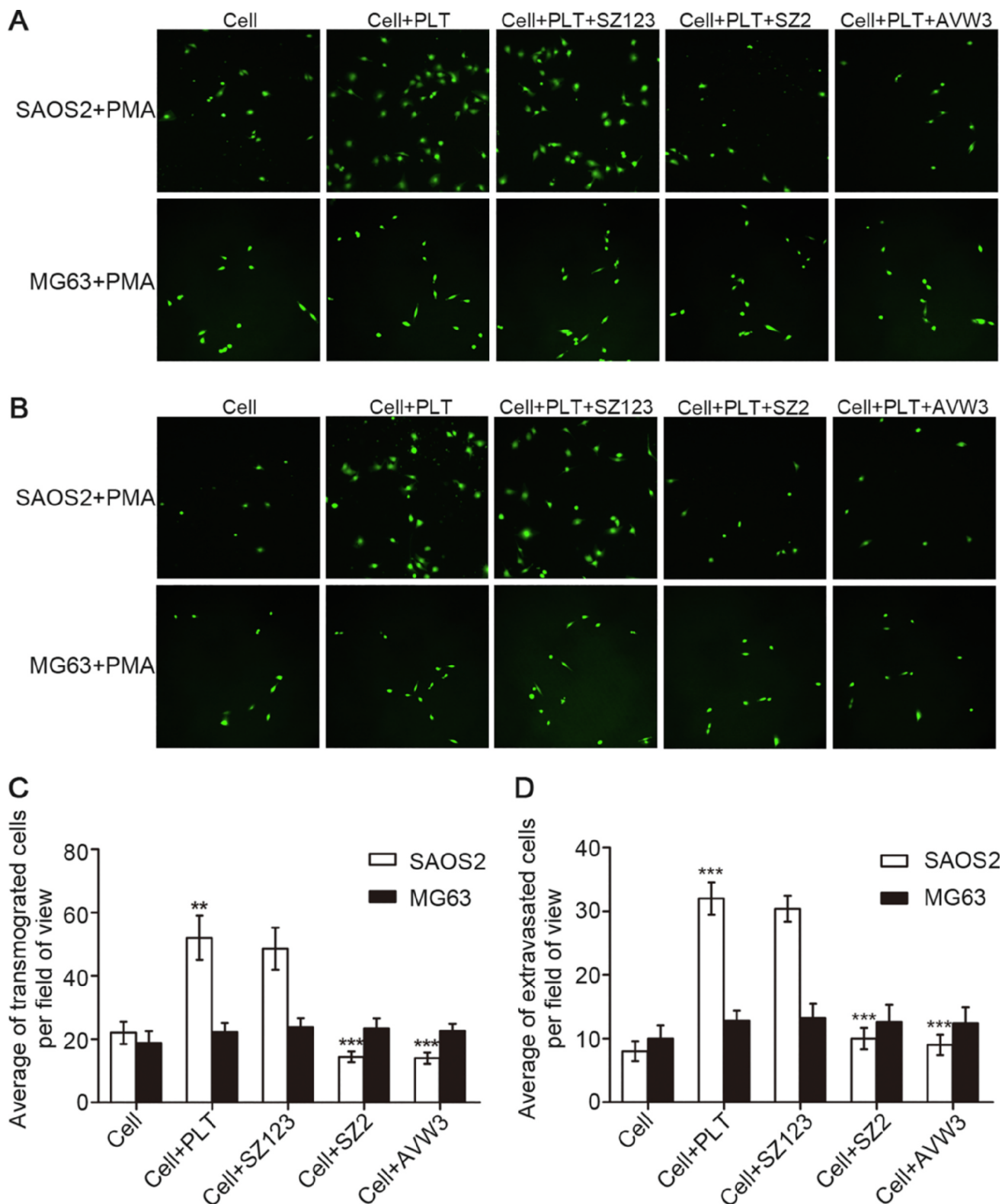


Fig. 5. Inhibition effect of VWF-GPIIb pathway blocking antibodies in transmigration and invasion capacity of SAOS2 cells treated with PMA. (A) the microscopic images of SAOS2 and MG63 (negative control) cells treated with PMA and stained with CFSE (green) that transmigrated through the membrane barrier in Cell, Cell + PLT, Cell + PLT + SZ123, Cell + PLT + SZ2 and Cell + PLT + AVW3; (B) the microscopic images of SAOS2 and MG63 (negative control) cells treated with PMA and stained with CFSE (green) that invaded through the matrigel membrane barrier in Cell, Cell + PLT, Cell + PLT + SZ123, Cell + PLT + SZ2 and Cell + PLT + AVW3; (C, D) quantification of transmigrated and invaded cells. Mean \pm SD is shown for three separate experiments. **P < 0.01, ***P < 0.001. (For interpretation of the references to colour in this figure legend, the reader is referred to the web version of this article.)

metastasis [23–26]. Platelet-mediated primary hemostasis has also been demonstrated to be required for hematogenous metastasis in a variety of experimental models [27,28]. Regarding the role of VWF in cancer metastasis, we hypothesized that the increase of VWF expression in OS cells may contribute to the enhancement of platelet adhesion through the VWF-GPIIb pathway, thus promoting the metastasis of OS. Our experimental results showed that platelets could adhere to SAOS2 cells through the VWF expressed on the cell membrane. Furthermore, this process could be significantly inhibited by the addition of SZ2, a monoclonal antibody against platelet GPIIb [29], as well as AVW3, an antibody targeting the A1 domain of VWF [30] under both static and shear stress conditions. These results demonstrated that platelet adhesion to SAOS2 cells is mediated by the binding between VWF A1 and GPIIb α of platelets, a molecular mechanism similar to that of thrombosis. Interestingly, the antibody SZ123, which targets the VWF A3 domain [31], could not inhibit the adhesion between platelets and SAOS2 cells under static condition, but showed an obvious inhibitory effect under shear stress condition. VWF can bind to exposed sub-endothelium collagen matrix through its A3 domain and to the platelet receptor GPIIb α through the A1 domain under shear stress condition *in vivo*. Based on our results, we hypothesized that the collagen binding site of the A3 domain is not open under static condition, thus the antibody could not play an inhibitory effect. However, under shear stress condition, the A3 domain could be exposed and the binding of SZ123 to the A3 domain may mask the binding site of VWF A1 to GPIIb α , thereby inhibiting the VWF-platelet interaction indirectly. Subsequently, our results demonstrated that SAOS2 cell-platelet aggregates further enhanced the migration and invasion capacities of tumor cells. Antibodies that block the VWF-GPIIb pathway also decreased numbers of SAOS2 cells that migrated and invaded to the lower layers. In contrast of results of the negative control MG63 cells, we hypothesized that due to the collagen-VWF-GPIIb axis interaction may play a role in OS metastasis, the differences between collagen and VWF expressed in the two OS cell lines may result in their different behaviors in the analyses. Studies have shown that the expression of various types of collagen is increased during OS metastasis [10,11]. In an *in vitro* cell model, different OS cells secreted different types of collagen. Type I collagens, are more abundant in SAOS2 cells, while Type II and type III collagens show higher expression level in other type OS cells [12]. This feature of SAOS2 cells may be due to the fact they are mature OS cells [13]. Combined with our results, it was hypothesized that the high expression of Type I collagen and VWF in SAOS2 cells may be the reason for their different behaviors.

In summary, our study demonstrates that the SAOS2 cell-derived VWF promotes platelet-induced metastasis of OS cells through activation of the VWF-GPIIb axis *in vitro*. Our results indicate that targeting the pathway may be an effective antitumor metastasis strategy and further enrich the mechanism of OS metastasis. However, until now it is difficult for the pathway to be applied to the clinical treatment because so far there is no research to deeply explore the difference between VWF expressed in OS cells and VWF derived from Ecs and platelets. Therefore, targeting OS cell-derived VWF is the key points and difficulties for the pathway applied to the clinical treatment in the future. Furthermore, animal model experiment and downstream molecular mechanism of this pathway in platelet-induced metastasis of OS are needed for the subsequent study.

5. Authors' contributions

The authors' initials are used. YZ contributed to the grant support conception, design of this project and critical revision of the manuscript. QW and MJ contributed to data acquisition and manuscript preparation. WL and LG contributed to diagnosis and evaluation of pathological sections. JG contributed to collecting patients' clinical data. FS and ZM contributed to operation of cell experiment. CR and JF revised and corrected the manuscript.

6. Ethics approval and consent to participate

Investigations abided by the Declaration of Helsinki and were approved by the Ethical Committee of the First Affiliated Hospital of Soochow University, Suzhou, China. Informed consent was obtained from individuals in accordance with the institutional ethics guidelines.

7. Consent for publication

All authors read and approved the final manuscript.

8. Availability of data and material

Data sharing not applicable to this article as no datasets were generated or analyzed during the current study.

Competing interests

All authors declare that they have no conflict of interest.

Funding

This study was supported by grants from National Natural Science Foundation of China (81873431), Jiangsu Provincial Natural Science Foundation (BK20181164), National Key Technology R&D Program of China (2012BA118B02) and National Institute of Health (HL128390, GM114731).

Acknowledgements

We thank Prof. Junlin Liu and Dr. Junliang Pan for critical reading of the manuscript. We appreciate the technical assistance of Liqian Xie and Yunxiao Zhao.

References

- [1] J.E. Sadler, *Biochemistry and genetics of von Willebrand factor*, *Annu. Rev. Biochem.* 67 (1) (1998) 395–424.
- [2] K.S. Sakariassen, P.A. Bolhuis, J.J. Sixma, Human blood platelet adhesion to artery subendothelium is mediated by factor VIII–Von Willebrand factor bound to the subendothelium, *Nature* 279 (5714) (1979) 636–638.
- [3] Z.M. Ruggeri, Von Willebrand factor, platelets and endothelial cell interactions, *J. Thromb. Haemost.* 1 (7) (2003) 1335–1342.
- [4] A. Mojiri, K. Stoletov, M.A. Lorenzana Carrillo, L. Willetts, S. Jain, R. Godbout, P. Jurasz, C.M. Sergi, D.D. Eisenstat, J.D. Lewis, N. Jahroudi, Functional assessment of von Willebrand factor expression by cancer cells of non-endothelial origin, *Oncotarget* 8 (8) (2017) 13015–13029.
- [5] J.A. SHAVIT, D.G. MOTTO, Coagulation and metastasis - an unexpected role for von Willebrand factor, *J. Thromb. Haemost.* 4 (3) (2006) 517–518.
- [6] K. Eppert, J.S. Wunder, V. Aneliunas, R. Kandel, I.L. Andrusis, von Willebrand factor expression in osteosarcoma metastasis, *Mod. Pathol.* 18 (3) (2005) 388–397.
- [7] E.G. Huijzinga, S. Tsuji, R.A. Romijn, M.E. Schiphorst, P.G. de Groot, J.J. Sixma, P. Gros, Structures of glycoprotein Ib alpha and its complex with von Willebrand factor A1 domain, *Science* 297 (5584) (2002) 1176–1179.
- [8] Z.M. Ruggeri, von Willebrand factor, perspectives series: cell adhesion in vascular biology, *J. Clin. Invest.* 99 (4) (1997) 559–564.
- [9] A. Bonnefoy, R.A. Romijn, P.A.H. Vandervoort, I. Van Rompaey, J. Vermylen, M.F. Hoylaerts, von Willebrand factor A1 domain can adequately substitute for A3 domain in recruitment of flowing platelets to collagen, *J. Thromb. Haemost.* 4 (8) (2006) 2151–2161.
- [10] F.D. Shapiro, D.R. Eyre, Collagen polymorphism in extracellular matrix of human osteosarcoma, *J. Natl Cancer Inst.* 69 (5) (1982) 1009–1016.
- [11] K. Minamitani, Establishment of an osteoblastic osteosarcoma cell line and effects of cell culture conditions on secretion of matrix metalloproteinases from the cultured osteosarcoma cells, *Kurume Med. J.* 47 (2) (2000) 115–124.
- [12] T. Wiklund, C. Blomqvist, L. Risteli, J. Risteli, E. Karaharju, I. Elomaa, Type I and type III collagen metabolites in adult osteosarcoma patients, *Br. J. Cancer* 73 (1) (1996) 106–109.
- [13] R. Muff, P. Rath, R.M. Ram Kumar, K. Husmann, W. Born, M. Baudis, B. Fuchs, Genomic instability of osteosarcoma cell lines in culture: impact on the prediction of metastasis relevant genes, *PLoS One* 10 (5) (2015) e0125611.
- [14] P. Picci, Osteosarcoma (osteogenic sarcoma), *Orphanet. J. Rare Dis.* 2 (1) (2007) 6.
- [15] J. Gill, M.K. Ahluwalia, D. Geller, R. Gorlick, New targets and approaches in osteosarcoma, *Pharmacol. Ther.* 137 (1) (2013) 89–99.
- [16] M.S. Isakoff, S.S. Bielack, P. Meltzer, R. Gorlick, Osteosarcoma: current treatment

- and a collaborative pathway to success, *J Clin Oncol* 33 (27) (2015) 3029–3035.
- [17] M. Kansara, M.W. Teng, M.J. Smyth, D.M. Thomas, Translational biology of osteosarcoma, *Nat. Rev. Cancer* 14 (11) (2014) 722–735.
- [18] L. Wang, P. Li, X. Xiao, J. Li, J. Li, H.-H. Yang, W. Tan, Generating lung-metastatic osteosarcoma targeting aptamers for in vivo and clinical tissue imaging, *Talanta* 188 (2018) 66–73.
- [19] A.J. Chou, E.S. Kleinerman, M.D. Krailo, Z. Chen, D.L. Betcher, J.H. Healey, E.U. Conrad III, M.L. Nieder, M.A. Weiner, R.J. Wells, R.B. Womer, P.A. Meyers, Addition of muramyl tripeptide to chemotherapy for patients with newly diagnosed metastatic osteosarcoma: A report from the Children's Oncology Group, *Cancer* 115 (22) (2009) 5339–5348.
- [20] D. Chen, Z. Zhao, Z. Huang, D.-C. Chen, X.-X. Zhu, Y.-Z. Wang, Y.-W. Yan, S. Tang, S. Madhavan, W. Ni, Z. Huang, W. Li, W. Ji, H. Shen, S. Lin, Y.-Z. Jiang, Super enhancer inhibitors suppress MYC driven transcriptional amplification and tumor progression in osteosarcoma, *Bone Res.* 6 (1) (2018) 11.
- [21] L. Toth, B. Nagy, G. Mehes, E. Laszlo, P.P. Molnar, R. Poka, Z. Hernadi, Cell adhesion molecule profiles, proliferation activity and p53 expression in advanced epithelial ovarian cancer induced malignant ascites—Correlation of tissue microarray and cytology microarray, *Pathol. Res. Pract.* 214 (7) (2018) 978–985.
- [22] J.F. Whitfield, J.P. Macmanus, D.J. Gillan, Calcium-dependent stimulation by a phorbol ester (PMA) of thymic lymphoblast DNA synthesis and proliferation, *J. Cell. Physiol.* 82 (2) (1973) 151–156.
- [23] P. Jurasz, D. Alonso-Escolano, M.W. Radomski, Platelet–cancer interactions: mechanisms and pharmacology of tumour cell-induced platelet aggregation, *Br. J. Pharmacol.* 143 (7) (2004) 819–826.
- [24] D. Stegner, S. Dütting, B. Nieswandt, Mechanistic explanation for platelet contribution to cancer metastasis, *Thromb. Res.* 133 (2014) S149–S157.
- [25] G.P. Gupta, J. Massagué, Platelets and metastasis revisited: a novel fatty link, *J. Clin. Invest.* 114 (12) (2004) 1691–1693.
- [26] J.S. Palumbo, K.E. Talmage, J.V. Massari, C.M. La Jeunesse, M.J. Flick, K.W. Kombrinck, M. Jirousková, J.L. Degen, Platelets and fibrin(ogen) increase metastatic potential by impeding natural killer cell-mediated elimination of tumor cells, *Blood* 105 (1) (2005) 178–185.
- [27] G.F. Nash, L.F. Turner, M.F. Scully, A.K. Kakkar, Platelets and cancer, *Lancet Oncol.* 3 (7) (2002) 425–430.
- [28] L.J. Gay, B. Felding-Habermann, Contribution of platelets to tumour metastasis, *Nat. Rev. Cancer* 11 (2) (2011) 123–134.
- [29] C.G. Ruan, X.P. Du, X.D. Xi, P.A. Castaldi, M.C. Berndt, A murine antiglycoprotein Ib complex monoclonal antibody, S22, inhibits platelet aggregation induced by both ristocetin and collagen, *Blood* 69 (2) (1987) 570–577.
- [30] D.J. Mancuso, P.A. Kroner, P.A. Christopherson, E.A. Vokac, J.C. Gill, R.R. Montgomery, Type 2M: Milwaukee-1 von Willebrand disease: an in-frame deletion in the Cys509-Cys695 loop of the von Willebrand factor A1 domain causes deficient binding of von Willebrand factor to platelets, *Blood* 88 (7) (1996) 2559–2568.
- [31] Y. Zhao, N. Dong, F. Shen, L. Xie, C. Ruan, Two novel monoclonal antibodies to VWFA3 inhibit VWF-collagen and VWF-platelet interactions, *J. Thromb. Haemost.* 5 (9) (2007) 1963–1970.